Int. J. Heat Mass Transfer. Vol. 20, pp. 475–486. Pergamon Press 1977. Printed in Great Britain

INTERNAL FORCED CONVECTION TO MIXTURES OF INERT GASES

D. M. McEligot,*† M. F. Taylor† and F. Durst*

(*Received* 28 *May* 1976)

Abstract—Mixtures of inert gases can be used to improve performance in closed gas turbine cycles. In the present work, heat transfer and wall friction parameters have been obtained numerically to demonstrate the effects of mixture composition and gas property variation for heating or cooling in regenerative heat exchangers of such cycles; the situation is modelled by laminar flow through short ducts with constant wall heat flux. For design predictions accounting for the effect of property variation, it is found that the property ratio method is better than the film temperature method for heat transfer while the latter method is preferable for apparent wall friction—with the proviso that the present definitions of the non-dimensional parameters be employed.

NOMENCLATURE

a, b, c, exponents for temperature-dependence of properties, equation (6);
c_p, specific heat at constant pressure;
D_h, hydraulic diameter (twice plate spacing);
G, average mass flux;
g_c, dimensional constant;
h, heat-transfer coefficient;
k, thermal conductivity;
L, length;
p, pressure;
p, q, exponents for property ratio method, equations (11) and (15);
T, absolute temperature;
u, axial velocity;
V_b, bulk velocity;
x, axial coordinate.

Greek symbols

$\varepsilon/\kappa, \sigma$, force constants in Lennard–Jones [6–12] potential;
μ, absolute viscosity;
ρ, density.

Dimensionless quantities

f, f_{ap}, apparent friction factor based on one-dimensional apparent wall shear stress, e.g. equation (13); f_a, lengthwise mean apparent friction factor;
$\bar{H}$, enthalpy, $(H - H_0)/(c_{p0} T_0)$;
L^+, length for velocity boundary layer, $4L/(D_h Re)$;
L^*, length for thermal boundary layer, $4L/(D_h Re\, Pr)$;
Nu, Nusselt number, hD_h/k;
$\bar{p}$, pressure, $2g_c \rho_0 p/G^2$;
Pr, Prandtl number, $c_p \mu/k$;
Q^+, wall heat flux, $q''_w D_h/(k_0 T_0)$;
Re, Reynolds number, GD_h/μ; Re_x, based on axial coordinate $\rho V_{b0} x/\mu$;
v^+, transverse velocity, $(1/4) vRe/V_{b0}$;
x^+, axial coordinate for velocity boundary layer, $4x/(D_h Re)$;
x^*, axial coordinate for thermal boundary layer, $4x/(D_h Re\, Pr)$;
$\bar{y}$, transverse coordinate, y/D_h.

Subscripts

a, overall average or mean value (lengthwise);
b, properties evaluated at bulk temperature;
cp, based on constant property idealizations;
e, in entry region;
f, based on film temperature, $(T_w + T_b)/2$;
fd, fully established or asymptotic value;
m, lengthwise mean value;
ref, reference;
w, properties evaluated at wall temperature;
x, properties evaluated at local temperature;
0, inlet conditions.

The circumflex (^) represents non-dimensionalization with respect to the value of the quantity at the inlet, e.g. $\hat{\rho} = \rho/\rho_0$.

1. INTRODUCTION

The closed Brayton cycle, or gas turbine cycle, has been suggested as an efficient, compact, versatile system for power plant and propulsion applications [1, 2]. With thermodynamic cycle studies, Bammert and Klein [3] showed that considerable savings in the total costs of a gas turbine cycle can be achieved by mixing helium with a heavier gas; the increase in density reduces the size of the turbomachines while the reduction in thermal conductivity increases the size of the heat exchangers so that an optimum occurs at an intermediate molecular weight. Approximate calculations indicate that when the heavier gas is another noble gas further improvements in heat-transfer performance are possible, compared to pure gases at the same pressure, temperature

*Institut für Hydromechanik und Sonderforschungsbereich 80, Universität Karlsruhe, D-7500 Karlsruhe, BRD.
†Aerospace and Mechanical Engineering Department, University of Arizona, Tucson, Arizona 85721, U.S.A.

and molecular weight [4]. However, the gaseous data and correlations for heat exchangers have been obtained with pure gases, primarily air, with negligible variation of the transport properties. Whether such results can be applied for mixtures of inert gases with temperature-dependent properties is a basic question which the present paper attacks.

In gas turbine cycles the regenerative heat exchanger is typically constructed of parallel plates, with short fins attached forming additional parallel surfaces. Consideration of the heat-transfer performance versus pumping power requirements of these heat exchangers usually results in design for operation in the laminar or transitional flow regime. For laminar flow heat exchangers, the streamwise length of the fins is shortened in order to take advantage of the increased heat-transfer coefficient of developing boundary layers by continually reinitiating the boundary layer. The thermal boundary condition is an approximately constant wall heat flux. As a guide to the effects of mixture composition and property variation in such geometries, the present paper—for a *first objective*—investigates the simultaneous development of laminar thermal and velocity boundary layers in the entry region of parallel plate ducts.

The following section briefly discusses related work which can be extended to provide improved guidance to the designer of regenerative heat exchangers for mixtures of noble gases. Section 3 summarizes pertinent knowledge of their transport properties and demonstrates the generalizations possible to reduce the analytical task. Since the consequent governing equations are non-linear and coupled, they are solved numerically as outlined in Section 4. The results of interest in design—lengthwise mean parameters—are presented in Section 5: first, the effect of composition at low heating rates and, then, the effects that the temperature-dependence of the transport properties cause on the heat-transfer parameters and the wall friction parameters, separately. Finally, the major conclusions are reiterated in the last section.

2. PREVIOUS WORK

In preliminary design studies for closed gas turbine systems, Vanco [4] estimated relative heat-transfer coefficients and pressure drop for binary mixtures of the inert gases with geometry held constant. For heat transfer he employed a constant property version of the Sieder–Tate relationship suggested by Kern [5]

$$Nu_m = 1.86Re^{1/3}Pr^{1/3}(D/L)^{1/3} = 2.95(L^*)^{-1/3}. \quad (1)$$

This relation is essentially a thermal entry correlation of the Leveque form [6] which strictly applies only for a linear velocity profile as in the wall region of a fully established flow. With long tubes the Nusselt number should become constant rather than tending to zero as in the above relationship. For pressure drop calculations, Vanco used the friction factor for fully developed flow. His approach is still prevalant in industrial design of laminar flow heat exchangers.

As shown later, one of the main effects of varying mixture composition is to vary the Prandtl number. If the velocity profile is fully established before heating commences, the function $Nu_m(L^*)$ should depend on geometry and thermal boundary condition and be independent of Pr since the non-dimensional variables can be defined so that Pr does not appear in the governing energy equation or its boundary conditions [7]. Since thermal and shear boundary layers grow at different rates when the Prandtl number is not unity, the solutions to the simultaneous entry problem will vary with Prandtl number. In a numerical analysis Hwang and Fan [8] have shown this variation to be significant at low values of L^* for constant wall heat flux and constant fluid properties. For the comparable constant wall temperature problem, Schlünder [9] suggests applying the Pohlhausen solution in the immediate entry as

$$Nu_{m,e} = 0.664(L^*)^{-1/2}Pr^{-1/6} \quad (2)$$

in continuous functions of the form

$$Nu_m = \sqrt[n]{(Nu_{fd}^n + Nu_{m,e}^n)} \quad (3)$$

for design computation.

Schade and McEligot [10] developed a numerical solution to examine the effect of air property variation for the simultaneous entry problem with strong heating or cooling applied to two parallel plates. They concluded that the local Nusselt number increases slightly and local friction factors increase severely with heating. To engineers accustomed to constant property analyses, the occurrence of a large change in friction factor and pressure drop while the Nusselt number is changing only slightly might be surprising. Schade and McEligot showed that such comparisons are sensitive to the choice of the temperature at which the properties in the non-dimensional parameters are evaluated and that use of the constant property idealization can lead to either dangerous or conservative design, depending on the application.

For the heat exchanger applications, designers employ mean parameters and resort to empirical methods to correct for fluid property variation [11]. The two most common schemes are the reference temperature method and the property ratio method [12]. Based on experiment and approximate analysis, Kays recommends exponents for the latter method for various geometries and fluids. However, despite the ready availability of appropriate numerical methods for laminar flows for over a decade [13], these empirical correlations have not been refined and the question as to which is the more accurate method has not been answered. Accordingly, a *second objective* of the present paper is to examine this question and, if possible, to improve the exponents used in the property ratio method for the parallel plate geometry and constant wall heat flux.

3. TRANSPORT PROPERTIES OF NOBLE GAS MIXTURES

While real gas properties can be employed in the numerical analysis in tabular or equation form directly, it is advantageous to exploit the similarities between different mixtures to reduce the number of computa-

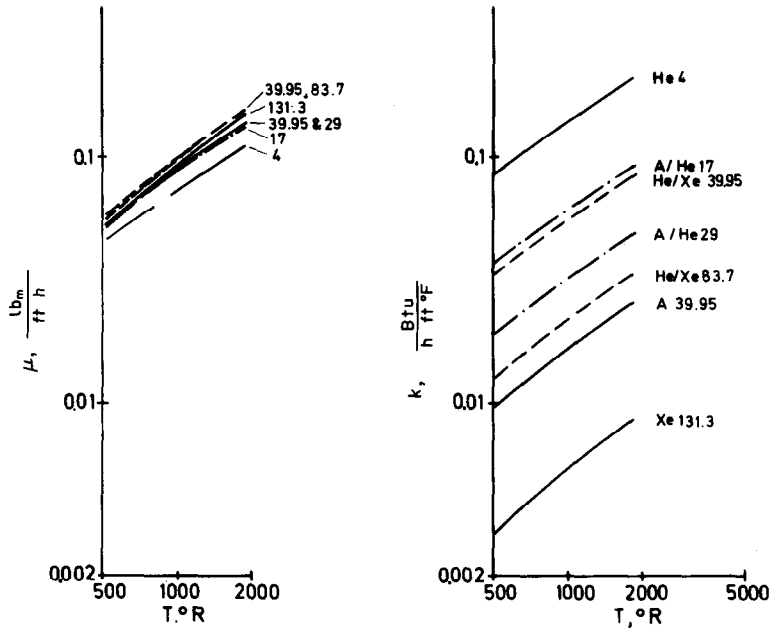

FIG. 1. Transport properties of noble gas mixtures. Number indicates molecular weight of mixtures.

tions necessary to cover the range of conditions of interest. Thus, if their behaviour can be generalized, fewer variations of parameters are required and the results are more concise and have greater usefulness. Accordingly, this section summarizes our knowledge of the pertinent transport properties. In conjunction with the following section it demonstrates that, as a first approximation, the variation in mixture composition can be reflected in the analysis in terms of a single variable parameter, the inlet Prandtl number.

The Lennard–Jones (6–12) potential can be employed in the Chapman–Enskog kinetic theory to predict thermal conductivity, viscosity and Prandtl number of binary mixtures of the inert gases [14]. There has been considerable experimental study of the pure gases, particularly helium and argon, but few data on their mixtures exist to check the predictions.

With force constants, ε/κ and σ, as suggested by Hirschfelder, Curtiss and Bird [14] the prediction of the helium viscosity falls about 8% below the data of Dawe and Smith [15] and Kalelkar and Kestin [16] at temperatures around 900 °C. Likewise, the predicted thermal conductivity is about 9% lower than the measurements of Saxena and Saxena [17] up to 1100 °C. Similar discrepancies occur for xenon, but agreement with argon data is close. In general, agreement is good near room temperature for these gases.

Thornton [18] measured viscosity of the helium/xenon system at 20 °C. His data agree with the predictions to within a few percent. On the other hand, the thermal conductivities obtained by Mason and von Ubish [19] at 520 °C show an increasing divergence from the predicted curve as the fraction of helium is increased. Using force constants suggested by DiPippo and Kestin [20] for the helium component, instead of those of Hirschfelder, Curtiss and Bird, leads to essential agreement with the recommended value from the Thermophysical Properties Research Center [21].

Thermal conductivity and viscosity are presented against logarithmic coordinates in Fig. 1 for helium, xenon, argon and some of their binary mixtures. These values are based on the Lennard–Jones (6–12) potential with the force constants $\sigma = 2.158$, 3.292 and 4.055 A, $\varepsilon/\kappa = 86.20$, 152.75 and 229 °K for helium, argon and xenon, respectively. The xenon values are from Hirschfelder, Curtiss and Bird and the others from DiPippo and Kestin.

Viscosities of the noble gases and their mixtures differ only slightly with molecular weight (composition). The variation with temperature is approximately the same for all. Using an idealized temperature dependence,

$$(\mu/\mu_{\text{ref}}) = (T/T_{\text{ref}})^a \tag{4a}$$

one finds the exponent "a" ranging from 0.7 to 0.8. On the other hand, the values of the thermal conductivity vary over an order of magnitude from xenon to helium. Again the temperature dependence is about the same for each and can be idealized as

$$(k/k_{\text{ref}}) = (T/T_{\text{ref}})^b. \tag{4b}$$

For the mixtures the exponent "b" is typically slightly less than "a" and ranges from about 0.7 to 0.75. As a first approximation, "a" and "b" could be taken as equal and the same value could be used for each of the mixtures. The specific heat is independent of temperature but varies with composition.

Perhaps the main surprise is the Prandtl number variation of the mixtures. Argon/helium and xenon/helium are shown in Fig. 2; the other mixtures yield curves of the same shape. The temperature dependence is almost negligible since the power law exponents for k and μ differ so little. The Prandtl number of the pure gases is 2/3. However, each binary system shows a minimum at intermediate concentrations (molecular weight); for xenon/helium it is $Pr \approx 0.22$ at room temperature and is particularly broad. Other Prandtl

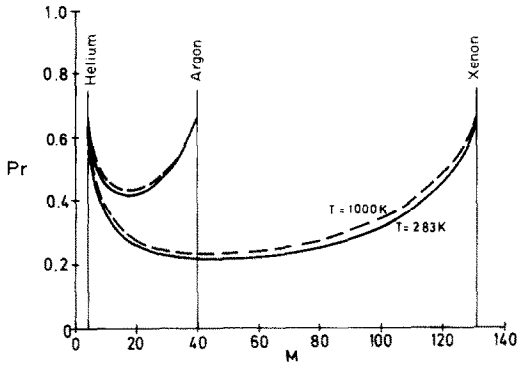

FIG. 2. Prandtl number variation with concentration (molecular weight).

number minima are: krypton/helium, 0.32; argon/helium, 0.42; krypton/neon, 0.53; xenon/argon, 0.57. Thus, Prandtl numbers in the range 0.5 to 2/3 can be obtained with several choices of binary mixture and concentration.

4. ANALYSIS

The details of the numerical analysis are straightforward and effectively the same as other methods for solution of coupled parabolic partial differential equations (e.g. [22]) so only the essentials will be outlined here. The number of parameters which must be varied to describe the range of conditions possible is determined by examination of the non-dimensional equations governing the problem.

Under the steady, internal boundary layer approximations—plus the assumptions that (a) mixture concentration remains constant, (b) Mach number $\ll 1$, (c) $RePr \gtrsim 100$, and (d) natural convection is negligible—the governing equations can be written.

Continuity:

$$\frac{\partial \hat{\rho}\hat{u}}{\partial x^+} + \frac{\partial \hat{\rho} v^+}{\partial \bar{y}} = 0, \tag{5a}$$

x-momentum:

$$\hat{\rho}\hat{u}\frac{\partial \hat{u}}{\partial x^+} + \hat{\rho} v^+ \frac{\partial \hat{u}}{\partial \bar{y}} = -\tfrac{1}{2}\frac{\mathrm{d}\bar{p}}{\mathrm{d}x^+} + \tfrac{1}{4}\frac{\partial}{\partial \bar{y}}\left(\hat{\mu}\frac{\partial \hat{u}}{\partial \bar{y}}\right), \tag{5b}$$

Energy:

$$\hat{\rho}\hat{u}\frac{\partial \overline{H}}{\partial x^+} + \hat{\rho} v^+ \frac{\partial \overline{H}}{\partial \bar{y}} = \frac{1}{4Pr_0}\frac{\partial}{\partial \bar{y}}\left(\hat{k}\frac{\partial \hat{T}}{\partial \bar{y}}\right), \text{ and} \tag{5c}$$

Integral continuity:

$$\int_0^{\bar{y}=1/2} \hat{\rho}\hat{u}\,\mathrm{d}\bar{y} = \tfrac{1}{2}. \tag{5d}$$

A circumflex ($\hat{}$) represents non-dimensionalization with respect to the value of the quantity at the entrance.

The gas properties may be idealized as:

$$\hat{\rho} = \frac{\bar{p}}{\bar{p}_0 \hat{T}}; \quad \hat{\mu} = \hat{T}^a; \quad \hat{k} = \hat{T}^b; \quad \hat{c}_p = \hat{T}^d. \tag{6}$$

Initial conditions are: $\hat{T}(0, \bar{y}) = 1$, $\bar{p}_0$ specified and $\hat{u}(0, \bar{y}) = 1$, i.e. uniform entry. Boundary conditions are (1) the nonslip condition for velocities, (2) constant wall heat flux,

$$-\left(\hat{k}\cdot\frac{\partial \hat{T}}{\partial \bar{y}}\right) = Q^+ \tag{7}$$

and (3) symmetry of the flow and boundary conditions with respect to the centre plane.

Examination of equations (5)–(7) shows the free parameters of the mathematical statement are Pr_0, Q^+, $\bar{p}_0$ and the property exponents a, b and d. For the present paper a and b are taken as 0.75, d as zero and $\bar{p}_0$ is set sufficiently high that the Mach number is small in the range of interest. The parameters Pr_0 (corresponding to the mixture molecular weight) and Q^+, the heating rate, remain variable.

The problem is solved numerically with program BAND, developed by Greif and McEligot [23] for flows between parallel plates with thermal radiative interaction using a band absorptance model. For the present calculations the capability to handle thermal radiation was suppressed, but property variation was included by choosing non-zero values of the exponents a and b. The numerical program is a finite control volume analysis using implicit algebraic equations to represent the governing equations; these equations are iterated at each axial step to treat their coupling and the nonlinear terms.

Mesh spacing increases in both the transverse and axial directions. For the results reported here, 81 transverse nodes were employed with the first usually at $(y/D_h) = 0.001$, and longitudinally there were 20 steps per decade normally starting at $x_0 = 10^{-5}$. As noted by Worsoe-Schmidt and Leppert [13] the boundary-layer approximations are not appropriate for $x^* < 10^{-3}$ so no results are reported for the initial two axial decades. Prior tests have shown convergence within 2% for Nu and within about 1% for f_{ap} with this grid.

5. RESULTS

Predictions have been obtained for the ranges $0.2 \leqslant Pr \leqslant 2/3$, corresponding to the Prandtl number variation from mixtures to pure gases, and $-2 \leqslant Q^+ \leqslant 100$. For $Q^+ \leqslant 10$, $\bar{p}_0$ was taken as 10^3 giving an inlet Mach number of 0.035 while at higher Q^+, $\bar{p}_0 = 10^4$ for $M_0 = 0.011$. Pertinent wall parameters are listed for a number of representative conditions in Table 1. More complete tabulations are available in [24].

With heating at a constant wall heat flux, the local bulk temperature increases continuously; with constant specific heat this increase is linear. The viscosity increases with temperature, so the local bulk Reynolds number (GD_h/μ_{bx}) decreases in the axial direction and the flow would be expected to remain laminar. Density is inversely proportional to temperature so the flow accelerates as it is heated, also normally a stabilizing influence. This continuous acceleration prohibits the occurrence of invariant velocity and temperature profiles. The wall temperature is larger than the bulk temperature in order to transfer energy to the gas so, at a given cross-section, the viscosity and thermal conductivity will be higher near the wall and the density

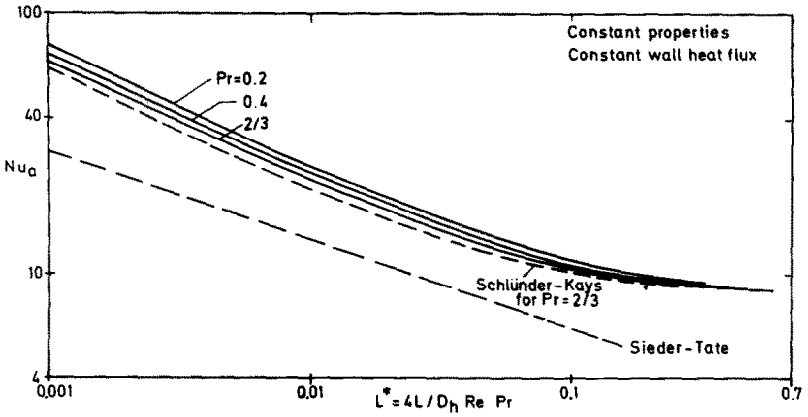

FIG. 3. Mean heat-transfer predictions under constant properties idealization.

will be lower. Consequently, parameters defined in terms of wall properties will have different values than those using bulk properties in their definition. While the increase in viscosity is expected to increase the wall shear stress and decrease the velocity near the wall, thus increasing thermal resistance, the increase in thermal conductivity is a factor tending to reduce thermal resistance. Likewise, the expansion due to reduced density counteracts the decrease due to viscosity to some extent. Near the entrance, the increased viscosity and decreased density at the wall augment the non-slip condition causing transverse flow away from the wall; this flow also carries thermal energy. Further downstream the transverse flow decreases. (These various effects are reversed with cooling.) While the individual effects of these phenomena can be forecast in some cases, their combined effect is not obvious and may vary with geometry. Since density, viscosity and thermal conductivity variations are all of the same order of magnitude, none dominates in such a way that a single-parameter, closed-form analysis would appear feasible.

For the present study the presentation of results emphasizes mean parameters which are useful to design engineers; however, local Nusselt numbers and friction factors are included in the tables for those interested. With property variation, parameters can take a number of values depending on how the temperatures which are used to evaluate the pertinent properties are defined. To avoid later confusion in the use of these predictions it is necessary to be explicit in the definitions.

Local bulk temperature, T_{bx}, is the temperature corresponding to the total enthalpy flow at a cross-section, i.e. the socalled mixing cup temperature. Average bulk temperature, T_{ba}, is the arithmetic average of the local value at length L and the inlet value

$$T_{ba} = (T_{b0} + T_{bL})/2.$$

While an integral average is normally used for the average wall temperature in analyses it is not of use to the designer who lacks the detailed knowledge of $T_w(x)$; accordingly, we define T_{wa} as an arithmetic average

$$T_{wa} = (T_{w0} + T_{wL})/2$$

which becomes, for constant wall heat flux,

$$T_{wa} = (T_{b0} + T_{wL})/2.$$

(Thus, T_{wa} is lower than $\int T_w(x)\,dx/L$.) Then, in agreement with normal practise, an average film temperature is chosen as

$$T_{fa} = (T_{wa} + T_{ba})/2.$$

Comparable subscripting is used for identifying the temperature at which properties are evaluated, e.g. $\mu_{ba} = \mu(T_{ba})$, and similarly for non-dimensional parameters, $Re_{ba} = GD_h/\mu_{ba}$. Average pressure is also taken at the arithmetic average of inlet and exit, L. Other quantities will be defined later as used.

Predictions for constant fluid properties

For small heating rates or low temperature differences the constant properties idealization is often adequate for practical applications. For example, one sees in Fig. 1 that a 50 °C difference in temperature causes a change in thermal conductivity of about 17% at room temperature and 4% at 1000 °K. In Fig. 3 are plotted the mean Nusselt numbers vs non-dimensional length, $L^* = 4L/(D_h RePr)$, as obtained by setting the property variation exponents, a and b, at zero and holding $\hat{\rho} = 1$. The mean Nusselt number is defined in terms of the integral average heat-transfer coefficient as

$$Nu_a = \frac{h_a \cdot D_h}{k} = \frac{D_h}{kL}\int_0^L h(x)\,dx.$$

From Fig. 3 one sees that in the entry $Nu_a(L^*)$ increases as the Prandtl number is reduced by employing different inert gas mixtures. This increase is approximately 17% as Pr varies from 2/3 to 0.2. Since, for constant properties, the development of the shear boundary layer is a function of $x^+ = 4x/(D_h Re)$ and is independent of Prandtl number (i.e. it is a solution of equations (5a, b and d)), the velocity profile is more fully developed for $Pr = 2/3$ than for $Pr = 0.2$ at any specified value of L^*. Consequently, the increase in Nu_a coincides with a higher average velocity gradient, $(\partial u/\partial y)_a$, between 0 and L^*; with increased velocities near the wall an increase in heat-transfer parameters is reasonable.

Table 1. Local and mean wall parameters

$\frac{4x}{D_h PrRe_0}$	T_b/T_0	T_w/T_b	Nu_{bx}	$\frac{f \cdot Re_{bx}}{24}$	T_{wa}/T_{ba}	Nu_{ba}	$\frac{f_{ba} \cdot Re_{ba}}{24}$	$\frac{p_0 - p}{G^2/(2\varrho_c \rho_0)}$
				$Pr = 0.2$				
				$Q^+ = 100$				
0.001	1.10	3.12	40.1	19.5	2.11	74.2	34.3	—
0.0023	1.23	3.50	27.9	11.8	2.38	49.9	22.4	—
0.0055	1.55	3.48	18.8	7.38	2.50	32.7	13.2	—
0.01	2.00	3.09	14.3	6.05	2.39	24.1	9.41	—
0.023	3.30	2.19	10.4	4.51	1.92	15.7	6.46	—
0.055	6.50	1.42	9.08	2.20	1.36	11.0	3.76	—
0.01	11.0	1.18	8.61	1.53	1.16	9.51	2.42	—
0.02	21.0	1.06	8.36	1.27	1.06	8.58	1.76	—
				$Q^+ = 10$				
0.001	1.01	1.27	39.9	12.3	1.12	75.3	22.0	0.127
0.0023	1.02	1.35	27.4	8.63	1.18	51.0	15.2	0.217
0.0055	1.06	1.48	19.0	5.90	1.25	34.2	10.3	0.395
0.01	1.10	1.56	15.1	4.52	1.29	26.2	7.84	0.611
0.023	1.23	1.61	11.4	3.24	1.34	18.4	5.34	1.18
0.055	1.55	1.49	9.40	2.37	1.30	13.2	3.59	2.56
0.1	2.00	1.33	8.93	1.93	1.22	11.1	2.76	4.72
0.2	3.00	1.17	8.60	1.51	1.13	9.61	2.09	10.9
0.5	6.00	1.05	8.36	1.17	1.05	8.61	1.52	43.8
				$Q^+ = 0$, constant properties				
0.001	—	—	40.1	10.3	—	75.7	19.4	—
0.0023	—	—	27.5	6.64	—	51.3	12.9	—
0.0055	—	—	18.9	4.38	—	34.4	8.46	—
0.01	—	—	14.9	3.28	—	26.4	6.33	—
0.023	—	—	11.2	2.26	—	18.7	4.25	—
0.055	—	—	9.14	1.58	—	13.6	2.85	—
0.1	—	—	8.55	1.28	—	11.4	2.20	—
0.2	—	—	8.32	1.07	—	9.92	1.67	—
0.5	—	—	8.24	1.00	—	8.92	1.28	—
				$Q^+ = -2$				
0.001	1.00	0.950	40.1	9.46	0.975	75.7	18.8	0.0863
0.0023	1.00	0.927	27.5	6.21	0.963	51.4	12.4	0.128
0.0055	0.99	0.892	18.9	3.95	0.946	34.5	8.00	0.188
0.01	0.98	0.861	14.9	2.83	0.931	26.5	5.90	0.239
0.023	0.95	0.805	11.2	1.83	0.905	18.7	3.86	0.318
0.055	0.89	0.725	8.92	1.14	0.871	13.6	2.50	0.379
0.09	0.82	0.655	8.21	0.792	0.845	11.7	1.97	0.362
				$Pr = 0.4$				
				$Q^+ = 100$				
0.001	1.10	3.25	37.7	14.0	2.18	69.1	25.2	0.464
0.0023	1.23	3.65	26.4	9.34	2.46	46.7	16.6	0.900
0.0055	1.55	3.60	17.9	6.26	2.58	30.8	10.4	1.94
0.01	2.00	3.18	13.7	4.99	2.45	22.9	7.63	3.49
0.023	3.30	2.24	10.0	3.43	1.95	15.0	5.11	8.91
0.055	6.50	1.43	8.74	1.73	1.38	10.6	2.92	26.6
0.1	11.0	1.18	8.45	1.34	1.16	9.19	1.97	63.7
0.2	21.0	1.06	8.31	1.21	1.06	8.41	1.60	247.

Table 1.—*continued*

$\frac{4x}{D_h PrRe_0}$	T_b/T_0	T_w/T_b	Nu_{bx}	$\frac{f \cdot Re_{bx}}{24}$	T_{wa}/T_{ba}	Nu_{ba}	$\frac{f_{ba} \cdot Re_{ba}}{24}$	$\frac{p_0 - p}{G^2/(2g_c\rho_0)}$
				$Pr = 0.4$				
				$Q^+ = 0$, constant properties				
0.001	—	—	36.9	7.12	—	69.5	13.9	0.133
0.0023	—	—	25.5	4.75	—	47.2	9.22	0.204
0.0055	—	—	17.6	3.16	—	31.8	6.05	0.319
0.01	—	—	14.0	2.39	—	24.5	4.55	0.436
0.023	—	—	10.7	1.69	—	17.4	3.09	0.682
0.055	—	—	8.80	1.24	—	12.8	2.11	1.12
0.1	—	—	8.35	1.07	—	10.9	1.67	1.61
0.2	—	—	8.25	1.01	—	9.57	1.35	2.59
0.5	—	—	8.24	1.00	—	8.77	1.14	5.47
				$Pr = 2/3$				
				$Q^+ = 100$				
0.0013	1.13	3.51	32.1	10.1	2.33	57.7	17.1	0.657
0.0023	1.23	3.76	25.3	7.79	2.52	44.3	13.1	1.04
0.0055	1.55	3.70	17.3	5.41	2.64	29.4	8.55	2.25
0.01	2.00	3.24	13.3	4.32	2.50	21.9	6.42	4.09
0.023	3.30	2.27	9.73	2.85	1.98	14.5	4.30	10.7
0.055	6.50	1.44	8.58	1.52	1.38	10.28	2.47	33.1
0.1	11.0	1.18	8.38	1.27	1.17	9.02	1.76	85.1
0.2	21.0	1.06	8.28	1.20	1.06	8.33	1.53	373.
				$Q^+ = 10$				
0.001	1.01	1.28	34.7	6.71	1.14	65.0	12.1	0.216
0.0023	1.02	1.40	24.3	4.74	1.20	44.3	8.33	0.360
0.0055	1.05	1.53	17.1	3.39	1.27	30.0	5.71	0.638
0.01	1.10	1.62	13.7	2.72	1.32	23.1	4.43	0.975
0.023	1.23	1.66	10.6	2.09	1.36	16.5	3.16	1.87
0.055	1.55	1.52	8.88	1.62	1.32	12.1	2.26	4.16
0.1	2.00	1.35	8.53	1.41	1.23	10.3	1.84	8.03
0.2	3.00	1.18	8.37	1.27	1.13	9.12	1.55	21.0
0.5	6.00	1.05	8.29	1.11	1.05	8.40	1.33	112.
				$Q^+ = 0$, constant properties				
0.0013	—	—	30.9	4.82	—	57.7	9.52	0.198
0.0023	—	—	24.1	3.71	—	44.3	7.20	0.265
0.0055	—	—	16.8	2.50	—	30.0	4.74	0.417
0.01	—	—	13.4	1.93	—	23.2	3.58	0.573
0.023	—	—	10.3	1.40	—	16.6	2.46	0.906
0.055	—	—	8.64	1.09	—	12.3	1.73	1.52
0.1	—	—	8.29	1.01	—	10.6	1.42	2.27
0.2	—	—	8.24	1.00	—	9.40	1.21	3.87
0.5	—	—	8.24	1.00	—	8.70	1.08	8.67
				$Q^+ = -2$				
0.001	1.00	0.942	34.7	5.26	0.971	65.2	10.5	0.165
0.0023	1.00	0.916	24.1	3.46	0.958	44.4	6.94	0.246
0.0055	0.99	0.878	16.7	2.26	0.939	30.0	4.50	0.371
0.01	0.98	0.845	13.3	1.69	0.923	23.2	3.35	0.488
0.023	0.95	0.787	10.2	1.15	0.896	16.6	2.25	0.704
0.055	0.89	0.709	8.43	0.807	0.863	12.3	1.52	0.994
0.09	0.82	0.647	8.01	0.681	0.841	10.8	1.25	1.17

Also plotted in Fig. 3 is the Sieder–Tate correlation (1) which has been employed in practise for heat-transfer calculations in comparable situations. In addition to differing by as much as a factor of two in the range of interest, this calculation fails to show the proper trend with L^* except approximately in the limited range $0.01 < L^* < 0.1$. At $L^* \approx 0.001$ the mean Nusselt number varies as $(L^*)^{-0.47}$ rather than $(L^*)^{-1/3}$ as in the Sieder–Tate correlation. Failure of this correlation to account for Prandtl number dependence has been mentioned earlier.

Based on an integral/superposition method Kays [12] suggests that the local Nusselt number for the simultaneous growth of laminar external boundary layers can be predicted by

$$Nu_x = 0.453 Pr^{1/3} Re_x^{1/2} \tag{8}$$

for the thermal boundary condition of a constant wall heat flux. For the immediate entry where $T_{bx} \approx T_0$ and $V_{bx} \approx V_0$, this relation can be transformed to a mean Nusselt number

$$Nu_{m,e} = 0.906 Pr^{1/3} Re_{D_h}^{1/2} D_h^{1/2} / L^{1/2}. \tag{9}$$

In this case, equation (3), the form suggested by Schlünder [9], would become

$$Nu_a = [8.235^2 + 1.812^2/(Pr^{1/3} L^*)]^{1/2}. \tag{10}$$

This equation is shown in Fig. 3 for a pure gas, $Pr = 2/3$, and can be seen to agree with the numerical prediction within about 10%. For the mixtures agreement is as good or better; the comparisons are shown individually later.

It should be re-emphasized that while the increase in $Nu(L^*)$ is of the order of 15%, when replacing a pure gas by a xenon–helium mixture, the gain in heat-transfer coefficient is much greater. For example, taking equation (9) as an approximation for short fins in conjunction with Figs. 1 and 2, one can see that for a given geometry and Reynolds number the effect of replacing pure argon by a helium–xenon mixture is to increase the heat-transfer coefficient about 2.4 times.

Predictions of heat transfer with property variation

When fluid properties vary significantly due to high heating rates and related large temperature variations in the flow field, the numerical values of non-dimensional parameters such as Nu and Re depend on the temperature at which their properties are evaluated. Two methods of accounting for the property variation are common in practise: the film temperature approach and the property-ratio approach [12]. In the film temperature approach it is assumed that using properties evaluated at T_f will allow direct use of predictions obtained under the constant property idealization. In the property ratio approach the bulk temperature is used for the properties and the effect of heating is represented as

$$Nu/Nu_{cp} = (T_w/T_b)^p \tag{11}$$

for gases. The effectiveness of these two methods for heat-transfer predictions is examined in the present section; wall friction predictions are considered in the following section.

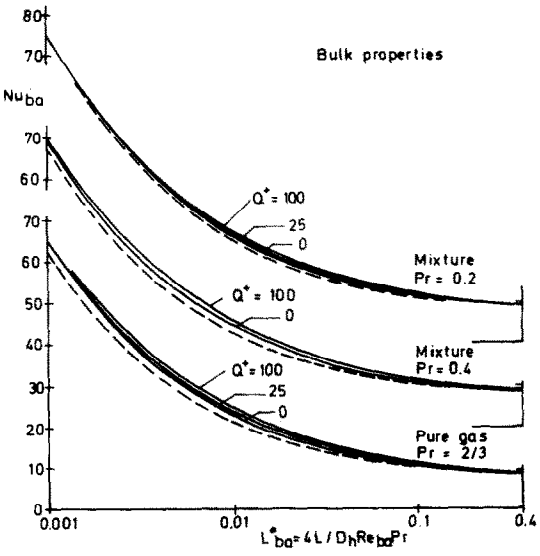

FIG. 4. Mean heat-transfer predictions in terms of bulk properties. Dashed line represents equation (10).

Figure 4 demonstrates the apparent effect of heating rate on the mean Nusselt number when the properties are taken at T_{ba}, i.e. the property ratio approach. Thus, L^*_{ba} is defined as $4L/(D_h Re_{ba} Pr) = 4Lk_{ba}/(c_p G D_h^2)$. The effect of heating the gas in a slight increase in Nu_{ba} compared to the prediction of Nu for constant properties ($Q^+ \to 0$) at the same value of L^*_{ba}. For a given value of Q^+, Nu_{ba} is increased more for the pure gases than for the mixtures, but this result is partially a consequence of the lower wall-to-bulk temperature reached by the gas with the lower Prandtl number. However, for $Q^+ = 100$, which leads to $(T_{wa}/T_{ba})_{max}$ around 2.5–2.7, the increase is only of the order of 5%. Thus, the exponent p in equation (11) would be about 0.05, which can probably be considered negligible for most practical cases. On the other hand, for $Q^+ = 100$ and $Pr = 2/3$ the local Nusselt number Nu_{bx} reaches a peak increase over the constant property prediction of about 25% at a location where $T_{wx}/T_{bx} \approx 3$ so the mean Nusselt number is affected even less than the local value.

To examine whether the film temperature approach is an improvement, the results are plotted in Fig. 5 with properties evaluated at the average film temperature, $Nu_{fa} = h_a D_h/k_{fa}$ and $L^*_{fa} = 4Lk_{fa}/c_p G D_h^2$. With this choice the mean Nusselt numbers decrease as the heating rate is raised. This effect is of approximately the same magnitude for the pure gases as for the mixtures with their lower Prandtl numbers. The most significant observation is that the reduction is about three times as great as the change when using bulk properties (Fig. 4) so there is no advantage in accuracy with the film temperature approach.

When heating the gas T_w and T_b both increase, T_w more rapidly in the entrance region and then both at approximately the same rate at larger distances. Consequently, T_w/T_b first increases and then approaches unity axially. Likewise, $Nu_{ba}(L^*)$ is first greater than

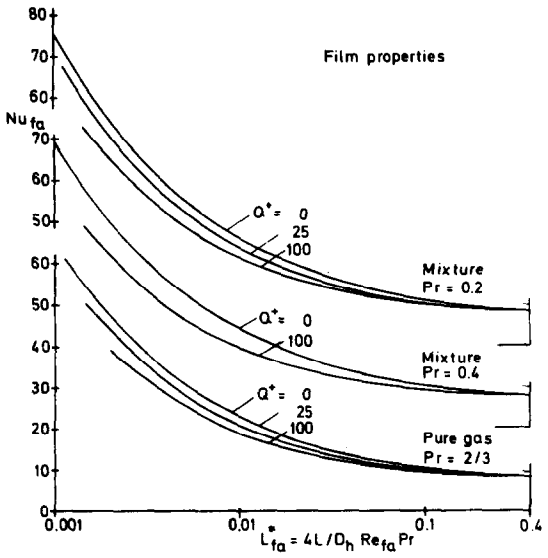

FIG. 5. Mean heat-transfer predictions in terms of film properties.

$Nu_{cp}(L^*)$ and then approaches $Nu_{cp}(L^*)$ downstream. In this situation correlations of the form of equation (11) make sense. In contrast, when cooling the gas—as on the opposite side of a regenerative heat exchanger—both temperatures decrease continuously such that, in the limit, T_w/T_b approaches zero or T_b/T_w approaches infinity. The relative property variation across the flow becomes greater downstream instead of less as in the heating situation. This limit is not likely to be of concern in a gas turbine cycle since the lowest temperature is set by the inlet temperature of the side to be heated, but might be a difficulty in cryogenic applications. In the cooling range covered in the scope of the present paper, $Nu_{ba}(L^*_{ba})$ remained sufficiently close to $Nu_{cp}(L^*)$ to neglect the difference.

If one calls equation (10) the Schlünder–Kays relation and plots it as a dashed line on each of the subfigures of Fig. 4, it may be seen that agreement with the constant property result is good for each case but successively better as Pr is reduced. Since $Nu_{ba}(L^*_{ba})$ is predicted so closely by $Nu_{cp}(L^*)$ it is worthwhile to improve the equation so it may be used by the designer over the range of interest. By adjusting the Prandtl number dependence of $Nu_{m,e}$ for better prediction at $L^* = 0.001$, one may obtain

$$Nu_a = [8.235^2 + 1.931^2/(Pr^{0.254}L^*)]^{1/2}. \quad (12)$$

This equation still is of the order of 5% lower than the numerical prediction near $L^* = 0.01$. For moderate heating rates it would be within about 10% of the numerical results and would be low; in heat exchanger design this would lead to units slightly longer than necessary. Alternatively, the constants in equation (12) could be optimized for another range at the expense of the accuracy of predictions in the immediate entry.

Prediction of wall friction with property variation

While most analyses presently available for developing flows present friction results in terms of the wall shear stress evaluated from the velocity gradient at the wall (f_s), this approach is not of use to the designer when the velocity profile is changing substantially, as in the entry or when a gas is heated. To predict the required pressure drop with a one-dimensional design procedure, one uses the "apparent" friction factor, f_{ap}, based on the wall shear determined by treating the momentum change as one-dimensional. The same treatment is often employed in experiments where size prohibits velocity profile measurements. Both methods of presentation can be chosen with numerical results; consequently, Bankston and McEligot [22] were able to demonstrate (a) the numerical values of f_s and f_{ap} can differ substantially and (b) discrepancies earlier thought to exist between experiments and analyses were primarily due to the differences in the definition used for the friction factors.

As with the heat-transfer results we concentrate in presenting a mean apparent friction factor,

$$f_a = -\frac{D_h}{4L}\frac{\rho}{G^2/2g_c}\underset{0}{\overset{L}{\triangle}}\left\{p + \frac{G^2}{\rho_b g_c}\right\}. \quad (13)$$

(The local apparent friction factor, f_x, appearing in the tables is defined in the analogous derivative form with d/dx replacing $(1/L)\underset{0}{\overset{L}{\triangle}}$.) When ρ_b is constant, the second term in brackets does not change and the definition reduces to that of Shah and London [7]. With constant fluid properties one solves equations (5a), (5b) and (5d) only, so the result is independent of Prandtl number and can be written as a single function $f_a(L^+)$ which approaches $f_a \cdot Re/24$ as L^+ becomes large. This function may be found tabulated in Table 1 or can be derived from earlier local results [10, 25]. For a continuous approximation, the approach of Schlünder can be used as in equation (13) to give

$$f_a \cdot Re/24 = \sqrt{(1 + 0.0788/L^+)} \quad (14)$$

which represents the numerical results well in the immediate entry but is 4–5% high in the range, $0.05 < L^+ < 0.2$.

With varying transport properties, the energy equation (5c) is coupled to equations (5a, b and d) via the temperature-dependent viscosity and density, so the wall friction also becomes a function of the Prandtl number and the heating rate. Again the question arises as to the better method of accounting for the fluid property variations. Predictions of friction are not as well behaved as heat-transfer parameters. In contrast to the heat-transfer results, direct use of the average bulk properties in f_a, Re and L^+ does not collapse the results nicely around the prediction based on constant properties; the main effect is to spread the curves towards larger L^+_{ba} as Q^+ increases.

The effect of heating rate on apparent wall friction is presented in Fig. 6 partially in terms of average bulk properties. That is, ρ_{ba} is used for the coefficient in equation (13) and Re_{ba} is defined as before but the non-dimensional length is based on inlet properties, i.e. L^+_0. With this representation heating increases $f_{ba} \cdot Re_{ba}$ considerably more than Nu_{ba} is raised at the

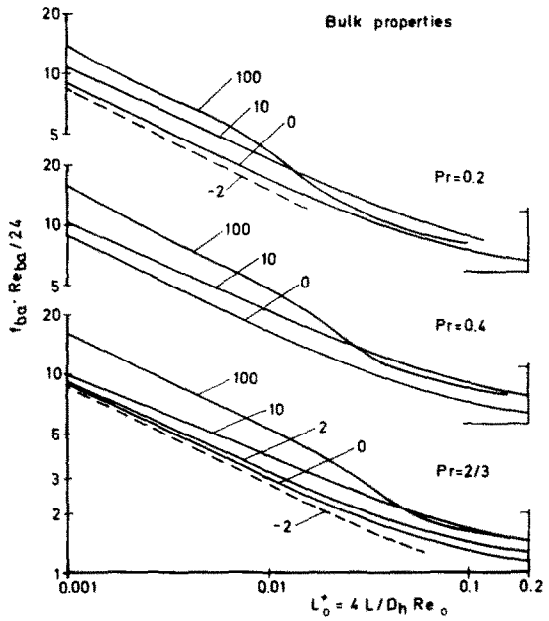

FIG. 6. Mean wall friction predictions in terms of bulk properties.

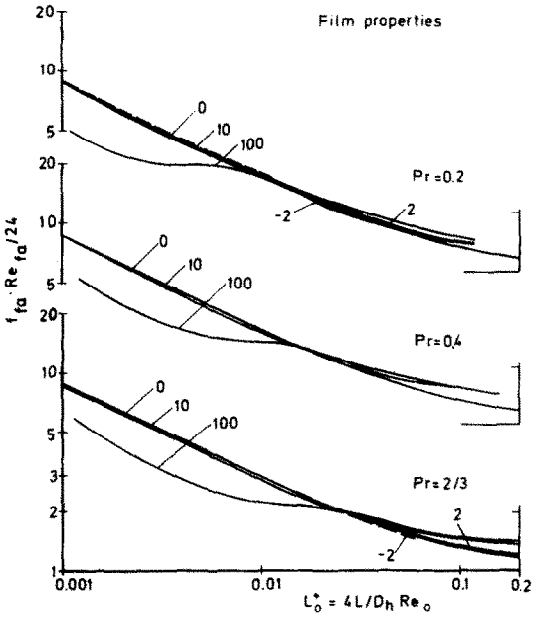

FIG. 7. Mean wall friction predictions in terms of film properties.

same level of Q^+. At lengths greater than $L^+ = 0.1$ the curves with heating approach the constant properties curve only slowly, although T_{wa}/T_{ba} is close to unity, as the heated entry continues to affect the integrated results far downstream. Close inspection of the trends for the highest heating rates shows that as Pr increases a convergence—from heated entry behavior towards agreement with constant property behavior—is moved further downstream. This effect corresponds to the difference in growth of the thermal boundary layer and shear boundary layer as the Prandtl number changes: $Nu(L^*)$ shows only a moderate effect of Pr, so for the same heating rate the value of T_w/T_b is almost the same at equal value of L^* rather than L^+, thus T_w/T_b approaches unity for $Pr = 0.2$ at earlier values of L^+ than for $Pr = 2/3$ and the variation of properties across the channel is less for $Pr = 0.2$ at the same L^+. While the friction predictions for heating approach the adiabatic prediction as L_{ba}^+ increases, those for cooling diverge; this result also corresponds to the trend of property variation since the ratio T_{ba}/T_{wa} increases downstream for cooling as described earlier in the section on heat transfer.

As with the heat-transfer results, the apparent effect of property variation on wall friction is sensitive to the choice of reference temperature. With average film temperature for the reference, the shape of the resulting curves differs from the shape with bulk temperature as reference. In Fig. 7 the product $f_{fa} \cdot Re_{fa}/24$ is plotted against L_0^+; ρ_{fa} is used in the coefficient in equation (13) and Re_{fa} is based on μ_{fa}. There is no advantage in comparison on the basis of L_{fa}^+ since results are shifted then further to the right (with heating) so that for $L^+ \gtrsim 0.01$ the difference from the adiabatic prediction is increased. For heating: the friction parameters are reduced for short lengths; then the predictions converge with and cross the constant properties curve and remain slightly greater at larger distances. In comparison to the bulk property predictions, the effects for short and long ducts are approximately the same magnitude with strong heating, but for intermediate lengths and for $Q^+ \gtrsim 10$ a display in terms of film properties shows significantly less variation. In the range $-2 < Q^+ < 2$ there is no significant effect of heating until L_0^+ approaches 0.1 with film properties and then the effect is only of the order of 5–10%. As is the case for bulk properties, the convergence towards the adiabatic prediction is at successively greater distances (L_0^+) as the Prandtl number increases, but for the same condition it is several times earlier with film properties. With cooling: the direction of the trends are reversed but for $Q^+ > -2$ they are essentially again negligible for entry problems.

It is not clear from Figs. 6 and 7 which approach is better: property ratio or film temperature. The property ratio approach would be represented as

$$(f_{ba} \cdot Re(L_0^+))/(f_a \cdot Re(L_0^+))_{cp} = (T_{wa}/T_{ba})^q \qquad (15)$$

so this quotient is plotted vs temperature ratio in Fig. 8 to examine the suitability of a single exponent. A

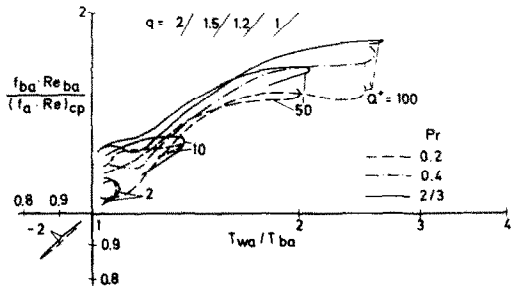

FIG. 8. Examination of property ratio method for mean wall friction.

complicated pattern appears. In contrast to the expectation of Kays and London [26], the general trend is a substantial increase with temperature ratio. There are slight differences with Prandtl number but the trends are mostly the same. An exponent q of the order of unity would overpredict the friction factor at the higher temperature ratios and underpredict it at lower values. For cooling, $q = 1$ is valid within a few percent. For moderate heating, the necessary value of q (i.e. the slope of a line from the origin on this logarithmic plot) varies with length L_0^+: it is approximately constant as the temperature ratio increases with length then increases gradually as the ratio drops for successively longer ducts. The latter effect is a consequence of the slow convergence of $f_{ba} \cdot Re_{ba}$ to the adiabatic curve for long ducts as discussed earlier. It is seen that a function $q(L_0^+, Q^+, Pr)$ would be necessary to describe the detailed behavior. For $Q^+ = 2$ and $L_0^+ < 0.6$, an exponent $q = 1.5$ would reduce the difference from the constant properties curve from 13% to a 7% discrepancy. With $Q^+ = 10$, $q = 1.2$ is a better approximation, but the discrepancy would still reach 20%. These comments and comparison of Figs. 6 and 8 suggest that the two methods have approximately the same overall accuracy for $Q^+ \lesssim 2$ with a slight advantage to the film properties approach for short ducts. For moderate heating—to $Q^+ = 10$—the film property method is clearly superior, while at higher heating rates both methods show regions where the simple correlations would mislead the designer substantially.

It is perhaps inconvenient for the designer to have one method perform better for heat transfer while the other is preferable for wall friction, but the difficulty should be negligible *provided* the present definitions of the parameters are used. Once the heat-transfer problem is solved for the wall temperature using average bulk properties, the average film temperature can be calculated from the results and can then be employed to predict the wall friction behavior.

Analytical correlations such as equations (12) and (14) are useful for parameter studies of systems and for initial sizing of components when hundreds to thousands of individual configurations may be calculated. When greater accuracy is needed in final design decisions—or if variable wall heat flux should be treated—the numerical analysis can be employed directly. With the direct application of the program, the question of definitions of the non-dimensional parameters is avoided; the engineer can choose definitions to suit his own convenience, including direct presentation in temperatures, pressure and lengths in units of his choice.

6. CONCLUSIONS

For heat transfer to mixtures of inert gases in short ducts formed of parallel plates, the following conclusions concerning the behavior of the mean parameters are warranted. In terms of appropriate non-dimensional variables and parameters, the effects of varying mixture concentration can be represented by variation of the inlet Prandtl number. These conclusions are based on the specific definition of parameters chosen in the present work; with strong heating rates the use of alternate definitions in the correlations can cause substantially different predictions of the heat-transfer coefficient and friction factor and, consequently, of the wall temperature and pressure drop.

(a) Under the constant property idealization, heat transfer and apparent wall friction parameters can be approximated by

$$Nu_a = [8.235^2 + 1.931^2/(Pr^{0.254} L^*)]^{1/2}$$

and

$$(f_a \cdot Re/24) = [1 + 0.0788/L^*]^{1/2}$$

to within 10% for L^* and L^+, respectively, greater than 0.001.

(b) For heat transfer in the range $-2 < Q^+ < 100$ the bulk properties/property ratio method of accounting for the effects of gas property variation—with exponent $p \gtrsim 0.005$—provides better predictions than the film temperature method.

(c) For wall friction in the range $-2 < Q^+ < 10$ the film temperature method is more accurate overall than the property ratio approach.

Acknowledgements—We are grateful to Dr. W. G. Harrach, AiResearch, Phoenix, Arizona, for suggesting the problem and providing the program to calculate the mixture properties. Dr. R. K. Shah, Harrison Radiator, Lockport, N.Y., provided valuable advice and Herr M. Simons helped compute. The work was supported by the Office of Naval Research (U.S.A.) and the Bundesministerium für Forschung und Technologie (BRD). The use of the Rechenzentrum, Universität Karksruhe and the University Computer Center, Arizona, is appreciated.

REFERENCES

1. K. Bammert, J. Rurik and H. Griepentrog, Highlights and future developments of closed-cycle gas turbines, ASME paper 74-GT-7 (1974).
2. E. A. Mock, Closed Brayton cycle system optimization for undersea, terrestrial, and space applications, von Kármán Institute for Fluid Dynamics, Brussels, Belgium (1970).
3. K. Bammert and R. Klein, The influence of He–Ne, He–N_2 and He–CO_2 gas mixtures on closed cycle gas turbines, ASME paper 74-GT-124 (1974).
4. M. R. Vanco, Analytical comparison of relative heat-transfer coefficients and pressure drops of inert gases and their binary mixtures, NASA TN-D-2677 (1965).
5. D. Q. Kern, *Process Heat Transfer*. McGraw-Hill, New York (1950).
6. P. M. Worsoe-Schmidt, Heat transfer in the thermal entrance region of circular tubes and annular passages with fully developed laminar flow, *Int. J. Heat Mass Transfer* **10**, 541–551 (1967).
7. R. K. Shah and A. L. London, Laminar flow forced convection heat transfer and flow friction in straight and curved ducts—a summary of analytical solutions, Tech. report 75, Mech. Eng., Stanford Univ. (1971).
8. C. L. Hwang and L. T. Fan, Finite difference analysis of forced convection heat transfer in entrance region of a flat rectangular duct, *Appl. Scient. Res.* **13A**, 401–422 (1964).
9. E. U. Schlünder, *VDI-Wärmeatlas*. VDI, Düsseldorf (1974).
10. K. W. Schade and D. M. McEligot, Cartesian Graetz problems with air property variation, *Int. J. Heat Mass Transfer* **14**, 653–666 (1971).
11. R. K. Shah, Personal communication, Harrison Radiator

Division, Lockport, N.Y. (1975).
12. W. M. Kays, *Convective Heat and Mass Transfer*, McGraw-Hill, New York (1966).
13. P. M. Worsoe-Schmidt and G. Leppert, Heat transfer and friction for laminar flow of a gas in a circular tube at a high heating rate, *Int. J. Heat Mass Transfer* **8**, 1281–1301 (1965).
14. J. O. Hirschfelder, C. F. Curtiss and R. B. Bird, *Molecular Theory of Gases and Liquids*. Wiley, New York (1964).
15. R. A. Dawe and E. B. Smith, Viscosities of the inert gases at high temperature, *J. Chem. Phys.* **52**, 693–703 (1970).
16. A. S. Kalelkar and J. Kestin, Viscosity of He–Ar and He–Kr binary gaseous mixtures in the temperature range 25–720 °C, *J. Chem. Phys.* **52**, 4248–4261 (1970).
17. V. K. Saxena and S. C. Saxena, Measurement of the thermal conductivity of helium using a hot-wire type of thermal diffusion column, *Br. J. Appl. Phys. (J. Phys. D.)* **1**, 1341–1351 (1968).
18. E. Thornton, Viscosity and thermal conductivity of binary gas mixtures: xenon–krypton, xenon–argon, xenon–neon and xenon–helium, *Proc. Phys. Soc.* **67**, 104–112 (1960).
19. E. A. Mason and H. von Ubisch, Thermal conductivity of rare gas mixtures, *Physics Fluids* **3**, 355–361 (1960).
20. R. DiPippo and J. Kestin, The viscosity of seven gases up to 500°C and its statistical interpretation, in *4th Symposium on Thermal Physical Properties*, pp. 304–313 (1969).
21. Y. S. Touloukian and C. Y. Ho, *Thermophysical Properties of Matter*. Plenum, London (1970).
22. C. A. Bankston and D. M. McEligot, Turbulent and laminar heat transfer to gases with varying properties in the entry region of circular ducts, *Int. J. Heat Mass Transfer* **13**, 319–344 (1970).
23. R. Greif and D. M. McEligot, Thermally developing laminar flows with radiative interaction using the total band absorptance model, *Appl. Scient. Res.* **25**, 234–244 (1971).
24. D. M. McEligot, M. F. Taylor and F. Durst, Laminar forced convection to mixtures of inert gases in parallel plate ducts. Tech. report 536, Institut für Hydromechanik, Universität Karlsruhe (June 1976).
25. J. R. Bodoia and J. F. Osterle, Finite difference analysis of plane Poiseuille and Couette flow development, *Appl. Scient. Res.* **10A**, 265–276 (1961).
26. W. M. Kays and A. L. London, *Compact Heat Exchangers*, 2nd edn. McGraw-Hill, New York (1964).

CONVECTION FORCEE INTERNE DANS LES MELANGES DE GAZ INERTES

Résumé—Les mélanges de gaz inertes peuvent être utilisés pour améliorer les performances des cycles fermés de turbines à gaz. Dans le présent travail, les paramètres de transfert thermique et de frottement pariétal ont été calculés numériquement afin de montrer les effets de la composition du mélange et des variations de propriétés physiques du gaz pour le chauffage et le refroidissement dans les échangeurs de chaleur à régénération présentant de tels cycles; la situation est modélisée à l'aide d'un écoulement laminaire à l'intérieur de conduites courtes avec flux pariétal constant. Pour les prévisions dans le domaine de la conception, qui tiennent compte de l'effet des variations de propriétés physiques, il s'avère que la méthode du rapport des propriétés est meilleure que la méthode de la température de film pour le transfert de chaleur tandis que cette dernière méthode est préférable pour la tension pariétale apparente—à la condition que les présentes définitions et paramètres adimensionnels soient utilisés.

ERZWUNGENE STRÖMUNG VON EDELGASGEMISCHEN IN KANÄLEN

Zusammenfassung—Der Einsatz von Edelgasgemischen in geschloseenen Gasturbinenanlagen kann Betriebsverbesserungen herbeiführen. In der vorliegenden Arbeit sind Wärmeübergangskoeffizienten und Reibungsbeiwerte angegeben, die numerisch errechnet wurden, um den Einfluß der Gemischzusammensetzung und der Gaseigenschaften auf den Wärmeaustausch im Rekuperator einer solchen Anlage zu ermitteln. Die wirklichen Verhältnisse wurden durch eine sich in kurzen Kanälen entwickelnde laminare Strömung mit konstantem Wärmeübergang simuliert. Die vorliegenden Berechnungen ergaben für die in der Praxis oftmals angewandten Ingenieurformeln, die die thermodynamischen Eigenschaften berücksichtigen, daß der Wärmeübergang besser mit einer Methode berechnet wird, in der die Stoffwerte des wandfernen Strömungsmediums eingesetzt werden, als mit der Filmtemperaturmethode. Die letztere ist jedoch für Berechnungen der Reibungswerte vorzuziehen, vorausgesetzt, daß die in der Arbeit definierten dimensionslosen Größen verwendet werden.

ВНУТРЕННЯЯ ВЫНУЖДЕННАЯ КОНВЕКЦИЯ В СМЕСЯХ ИНЕРТНЫХ ГАЗОВ

Аннотация — Смеси инертных газов могут использоваться для улучшения рабочих характеристик газовых турбин с замкнутыми циклами. Найдены численные значения характеристик теплопереноса и трения на стенке, показывающие влияние состава смеси и изменения свойств газа на процесс нагрева или охлаждения в регенеративных теплообменниках с замкнутыми циклами; процесс теплообмена рассматривается для случая ламинарного течения через короткие каналы при наличии постоянного теплового потока на стенке. Найдено, что в инженерных расчетах, учитывающих влияние изменения свойств газа, при определении теплопереноса метод, основанный на отношении свойств газа, лучше по сравнению с методом температуры пленки, в то время как последний предпочтительнее для рассмотрения трения на стенке при условии использования определений безразмерных параметров, данных в статье.